

# A Dielectric Model at a Frequency of 1.4 GHz for Frozen Mineral Soils in the Temperature Range $-1$ to $-30^{\circ}\text{C}$

V. L. Mironov<sup>1</sup>, L. G. Kosolapova<sup>1</sup>, Y. I. Lukin<sup>1</sup>, A. Y. Karavaysky<sup>1</sup>, and I. P. Molostov<sup>2</sup>

<sup>1</sup>Kirensky Institute of Physics SB RAS, Russia

<sup>2</sup>Altai State University, Russia

**Abstract**— A single-frequency dielectric model at 1.4 GHz for frozen mineral soils was developed, with the temperature and clay content varying from  $-1$  to  $-30^{\circ}\text{C}$  and 9.1 to 41.3%, respectively. The model is based on dielectric measurements of three typical soils (sandy loam, silt loam, and silty clay) collected in the Yamal peninsular. The refractive mixing model was applied to fit the data aggregates consisting of measured complex refractive indexes (CRI) for the three soils as a function of soil moisture at a fixed temperature. As a result, there were derived the parameters of the refractive mixing dielectric model as a function of temperature and texture. These parameters involve the maximum allowed gravimetric fraction of bound water and the CRIs of soil solids, bound soil water, and free soil water components, the latter being represented by capillary ice. The error of the dielectric model was evaluated by correlating the predicted complex relative permittivity (CRP) values of the soil samples with the measured ones. The coefficient of determination,  $R^2$ , and the root mean square error, RMSE, were estimated to be  $R^2 = 0.994$ ,  $\text{RMSE} = 0.22$  and  $R^2 = 0.988$ ,  $\text{RMSE} = 0.07$  for the real and imaginary parts of the CRP, respectively. These values are on the order of the dielectric measurement error itself. The proposed dielectric model can be applied in active and passive remote sensing techniques used in the Arctic areas, mainly for the SMOS, SMAP and Aquarius missions.

## 1. INTRODUCTION

The microwave radiometry from space of the earth surface at 1.4 GHz is currently becoming an effective tool for monitoring the soil moisture and temperature, with the SMOS and SMAP missions being the most demonstrative examples. The moisture and temperature dependent dielectric models of soils are a key element of the soil moisture and temperature retrieval algorithms based on the data of measured brightness temperatures. Earlier we created a texture- and temperature-dependent model of thawed mineral soils [1,2], which is currently included in both the SMOS and SMAP retrieval algorithms, alongside with the Dobson dielectric model [3]. As to the frozen mineral soils, there is the only model suggested by Zhang et al. [4], but this model has not been so far validated based of experimental data. In this paper, a single-frequency dielectric model at 1.4 GHz for frozen mineral soils was developed, with the temperature and clay content varying from  $-1$  to  $-30^{\circ}\text{C}$  and 9.1 to 41.2%, respectively.

## 2. CHARACTERIZATION OF SOILS

To develop the dielectric model we used three basic samples of the Arctic soils collected in Yamal peninsula (Russia). Dielectric measurements of soils were carried out in the range of soil moisture (from zero to field capacity), when the temperature changes from  $25^{\circ}\text{C}$  to  $-30^{\circ}\text{C}$ , and the frequency ranges from 0.05 to 15 GHz. The soil texture and mineral composition of measured soil samples are shown in Table 1. The mineral compositions of the soil samples are rather close to each other, though, their textures in term of clay content vary in the range from 9.1 to 41.2%.

Table 1: The soil texture parameters and mineral composition.

No.	Soil Type	<i>Soil Texture (%)</i>			<i>Mineral Composition</i>				
		Sand	Silt	Clay	Quartz (%)	Feldspar (%)	Plagio-clase (%)	Mica, chlorite (small impurity)	Smectite, Amphibol, Siderite (traces)
1	Sandy loam	41.4	49.5	9.1	40	30	30	Imp	Tr
2	Silt loam	40.4	39.0	20.6	70	15	5–10	Imp	Tr
3	Silty clay	1.6	57.1	41.3	60	20–25	5	Imp	Tr

### 3. DIELECTRIC MODEL

Dielectric measurements were carried out with the ZVK Rohde&Schwarz vector network analyzer. Preparation of soil samples and the measurement procedure are described in detail in [5]. The results of measurements are given in Fig. 1 in terms of the reduced CRIs,  $(n^* - 1)/\rho_d = (n - 1)/\rho_d + i\kappa/\rho_d$ , as a function of gravimetric moisture  $m_g$ , where  $n$  and  $\kappa$  are the refractive index and normalized attenuation coefficient, respectively, and  $\rho_d$  is the density of dry soil. The values of CRI,  $n^* = n + i\kappa$  and CRP,  $\varepsilon = \varepsilon' + i\varepsilon''$  are linked to each other by the following equations:

$$\varepsilon' = n^2 - \kappa^2, \quad \varepsilon'' = 2n\kappa. \quad (1)$$

The gravimetric moisture is determined as a ratio of the mass of soil water to that of the soil solids. In Table 2, are given the values of gravimetric moistures and dry soil densities for the measured soil samples. Using these data, the volumetric moistures,  $m_v$ , of the measured samples can be easily estimated,  $m_v = m_g\rho_d$ .

Table 2: Soil samples gravimetric moistures,  $m_g$  [g/g], and their respective soil densities,  $\rho_d$  [g/cm<sup>3</sup>].

Soil 1	$m_g$	0.004	0.005	0.012	0.023	0.039	0.047	0.052	0.061	0.072	0.091	0.096	0.101	0.117
	$\rho_d$	1.62	1.60	1.65	1.54	1.48	1.51	1.53	1.55	1.49	1.53	1.55	1.57	1.58
	$m_g$	0.135	0.156	0.165	0.182									
	$\rho_d$	1.65	1.86	1.67	1.65									
Soil 2	$m_g$	0.004	0.025	0.040	0.058	0.064	0.068	0.071	0.093	0.111	0.132	0.138	0.143	0.154
	$\rho_d$	1.52	1.36	1.41	1.29	1.33	1.36	1.34	1.43	1.44	1.45	1.50	1.55	1.46
	$m_g$	0.171	0.180	0.192	0.209	0.211								
	$\rho_d$	1.83	1.48	1.80	1.63	1.62								
Soil 3	$m_g$	0.004	0.047	0.058	0.061	0.066	0.077	0.080	0.085	0.097	0.111	0.129	0.136	0.144
	$\rho_d$	1.30	1.40	1.32	1.34	1.28	1.36	1.36	1.38	1.40	1.48	1.57	1.44	1.49
	$m_g$	0.154	0.164	0.182	0.205	0.233	0.236	0.263	0.274	0.280	0.289	0.298	0.300	0.315
	$\rho_d$	1.48	1.54	1.55	1.59	1.59	1.63	1.54	1.52	1.50	1.49	1.44	1.46	1.42

In the frame of the refractive mixing dielectric model as formulated in [5], the reduced CRI does not depend on the dry soil density:

$$\frac{n_s - 1}{\rho_d} = \left\{ \begin{array}{ll} \frac{n_m - 1}{\rho_m} + \frac{n_b - 1}{\rho_b} m_g & m_g \leq m_{g1} \\ \frac{n_m - 1}{\rho_m} + \frac{n_b - 1}{\rho_b} m_{g1} + \frac{n_i - 1}{\rho_i} (m_g - m_{g1}) & m_g \geq m_{g1} \end{array} \right\} \quad (2)$$

$$\frac{\kappa_s}{\rho_d} = \left\{ \begin{array}{ll} \frac{\kappa_m}{\rho_m} + \frac{\kappa_b}{\rho_b} m_g & m_g \leq m_{g1} \\ \frac{\kappa_m}{\rho_m} + \frac{\kappa_b}{\rho_b} m_{g1} + \frac{\kappa_i}{\rho_i} (m_g - m_{g1}) & m_g \geq m_{g1} \end{array} \right\} \quad (3)$$

The subscripts  $s$ ,  $d$ ,  $m$ ,  $b$ , and  $i$  (which are related to  $n$ ,  $\kappa$ , and  $\rho$ ) refer to the moist soil, dry soil, solid component of soil, bound water, and capillary ice, respectively.  $m_{g1}$  is the maximum allowed gravimetric fraction of bound water. The data aggregates consisting of measured complex refractive indexes (CRI) for the three soils as a function of soil moisture at a fixed temperature, as shown in Fig. 1, were fitted by the piecewise linear functions (2) and (3), using the software ORIGIN 9.0. As a result, there were derived 1) the maximum allowed gravimetric fractions of bound water,  $m_{g11}$ ,  $m_{g12}$ , and  $m_{g13}$ , pertaining to the soils 1, 2, and 3 (see Table 1); 2) the reduced CRIs for the bound water,  $(n_b - 1)/\rho_b$ ,  $\kappa_b/\rho_b$ , capillary ice,  $(n_i - 1)/\rho_i$ ,  $\kappa_i/\rho_i$ , and soil solids,  $(n_m - 1)/\rho_m$ ,  $\kappa_m/\rho_m$ , which were considered to be the same for all three soils. In Fig. 1, the values of  $m_{g11}$ ,  $m_{g12}$ , and  $m_{g13}$  that separate the range of bound water from that of capillary ice are shown with vertical dashed lines.

The above fitting procedure was performed for the measured data obtained at the temperatures of  $-1$ ,  $-2$ ,  $-3$ ,  $-4$ ,  $-5$ ,  $-10$ ,  $-15$ ,  $-20$ ,  $-25$ ,  $-30^\circ\text{C}$ , yielding the reduced CRI parameters  $(n_m - 1)/\rho_m$ ,  $(n_b - 1)/\rho_b$ ,  $(n_i - 1)/\rho_i$ ,  $\kappa_m/\rho_m$ ,  $\kappa_b/\rho_b$ , and  $\kappa_i/\rho_i$  as a function of temperature. While the

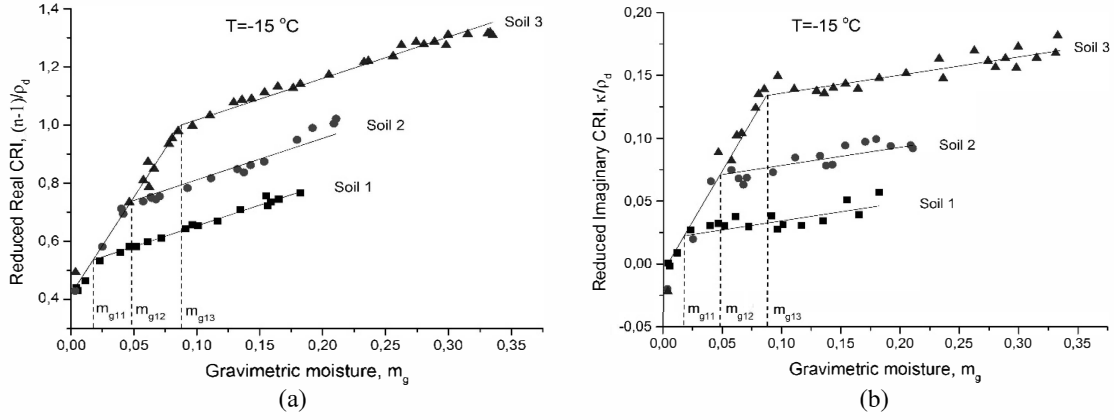


Figure 1: The reduced complex refractive index of the measured soils (symbols) at the temperature of  $-15^{\circ}\text{C}$  and wave frequency of 1.4 GHz as a function of gravimetric moisture. (a) The real part of the CRI, (b) the imaginary part of the CRI.

values of maximum allowed gravimetric fraction of bound water,  $m_{g1}$ , were derived with the applied fitting procedure as a function of both the temperature and percentage of clay content  $C$ , that is,  $m_{g1}(T, C)$ , which is shown in Fig. 2.

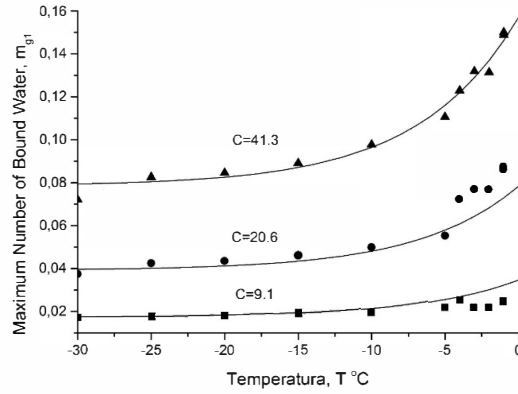


Figure 2: The maximum allowed gravimetric fractions of bound water as a function of temperature and soil texture (clay percentage,  $C\%$ ). The solid lines correspond to the fits as given by the first equation in (4). The symbols represent the fits obtained with the data like those given in Fig. 1 and the model given by (2) and (3).

In their turn, the temperature dependences of reduced CRI parameters  $(n_m - 1)/\rho_m$ ,  $(n_b - 1)/\rho_b$ ,  $(n_i - 1)/\rho_i$ ,  $\kappa_m/\rho_m$ ,  $\kappa_b/\rho_b$ , and  $\kappa_i/\rho_i$  were fitted with the exponent and linear functions, which are given by the formulas in (4). Further, the data aggregate for  $m_{g1}(T, C)$  shown in Fig. 2 was fitted using the theoretical model  $m_{g1}(T, C) = A(C)(1 + B\exp(T/T_d))$ . At that, parameters  $B$  and  $T_d$  were obtained using the data for all three soils, while the data for each individual soil were applied separately for deriving parameter  $A(C)$ , the values of which were finally fitted by a linear function of clay content  $C$ . The result of this fitting is given by the first equation in (4). Below, there are presented the dielectric model parameters as a function of soil temperature and texture.

$$\begin{aligned}
 m_{g1} &= 0.0019C(1 + 1.056\exp(T/6.77)) \\
 (n_m - 1)/\rho_m &= 0.415 - 0.0256\exp(T/3.57) \\
 (n_b - 1)/\rho_b &= 8.042 + 0.0921T \\
 (n_i - 1)/\rho_i &= 1.305 + 1.022\exp(T/4.02) \\
 \kappa_m/\rho_m &= 0 \\
 \kappa_b/\rho_b &= 1.654 - 0.258\exp(T/4.07) \\
 \kappa_i/\rho_i &= 0.204 + 0.00354T
 \end{aligned} \tag{4}$$

Equations (1)–(4) represent the temperature and texture dependent dielectric model for the CRP of frozen mineral soils at the frequency of 1.4 GHz. To calculate the CRP as a function of gravimetric

moisture or as a function of temperature using formulas in (1)–(4), one must assign the following variables: 1) dry soil density,  $\rho_d$  [g/cm<sup>3</sup>], 2) gravimetric moisture,  $m_g$  [g/g], 3) temperature,  $T$  °C, and 4) clay content in soil,  $C$  in %.

#### 4. VALIDATION OF THE DIELECTRIC MODEL

Verification of the model was carried out in three basic soils (on the basis of which it was created) and two independent soils (which have not been used to build the model). The mineral compositions of the independent soil samples are characterized by dominating presence of quartz (55–60%), feldspar (10%), and plagioclase (15–20%). While mica, chlorite, smectite, amphibol, and siderite are present in traces. By texture, the measured soils appeared to be classified into the following types: clay loam (sand 20.6%, clay 33.4%), and silty clay (sand 2.0%, clay 42.2%). As an example, Fig. 3 shows the results comparing the dielectric measurement of soil 2 (see Table 1) as a function of temperature, together with the respective predictions obtained with the use of the formulas in (1)–(4). As seen from Fig. 3, the calculated data are in good agreement with the measured ones. For independent soil the results of such a comparison is not much worse. To quantify the developed model error, we correlated the predicted CRPs with the set of measured CRPs relating to three basic and two independent soils with four moistures in all areas measured temperatures.

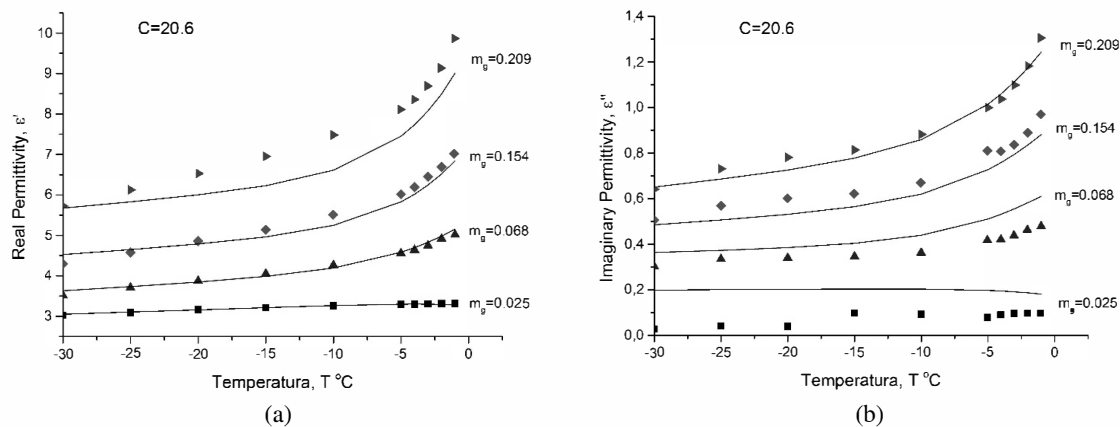


Figure 3: The CRP of moist soil as a function of temperature at the fixed gravimetric moistures  $m_g$  (given by inscriptions) and the frequency of 1.4 GHz. (a) The real part of the CRP,  $\epsilon'$ , (b) the imaginary part of the CRP,  $\epsilon''$ . The measured CRP values are represented by symbols. The solid lines correspond to the CRPs estimated with the dielectric model (1)–(4).

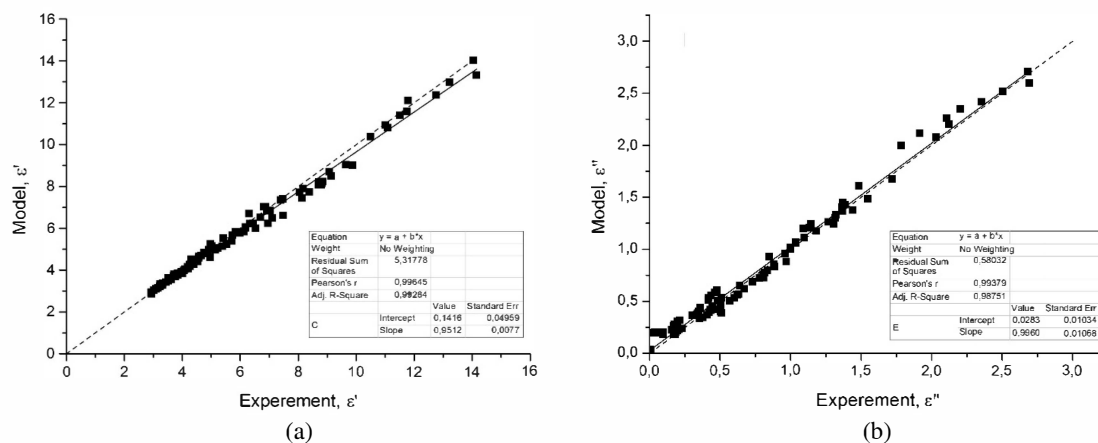


Figure 4: The calculated CRPs of moist soils as a function of the measured ones in the temperature ranges of  $-30^{\circ}\text{C} \leq T \leq -1^{\circ}\text{C}$ . (a) The real part of CRP,  $\epsilon'$ , (b) the imaginary part of CRP,  $\epsilon''$ . Bisectors represented by the dotted lines. Linear fits represented by the solid lines.

In Fig. 4, the predicted values of the real part (Fig. 4(a)) and the imaginary part (Fig. 4(b)) of the CRP are presented versus the respective measured values. To estimate the error, we calculated

separately the root mean square error (RMSE) and the coefficient of determination ( $R^2$ ) for the real and the imaginary parts of the CRP for the based soils ( $\text{RMSE}_{\varepsilon'_{\text{base}}}$ ,  $\text{RMSE}_{\varepsilon''_{\text{base}}}$ ,  $R^2_{\varepsilon'_{\text{base}}}$ ,  $R^2_{\varepsilon''_{\text{base}}}$ ) and independent soils ( $\text{RMSE}_{\varepsilon'_{\text{indep}}}$ ,  $\text{RMSE}_{\varepsilon''_{\text{indep}}}$ ,  $R^2_{\varepsilon'_{\text{indep}}}$ ,  $R^2_{\varepsilon''_{\text{indep}}}$ ). Their values presented in Table 3 are on the order of the dielectric measurement error itself.

Table 3: The values of Root Mean Square Errors (RMSE) and Coefficient of Determination ( $R^2$ ) for basic and independent soils.

$\text{RMSE}_{\varepsilon'_{\text{base}}}$	$\text{RMSE}_{\varepsilon'_{\text{indep}}}$	$\text{RMSE}_{\varepsilon''_{\text{base}}}$	$\text{RMSE}_{\varepsilon''_{\text{indep}}}$	$R^2_{\varepsilon'_{\text{base}}}$	$R^2_{\varepsilon'_{\text{indep}}}$	$R^2_{\varepsilon''_{\text{base}}}$	$R^2_{\varepsilon''_{\text{indep}}}$
0.22	0.27	0.07	0.12	0.994	0.992	0.988	0.963

## 5. CONCLUSIONS

A temperature- and texture-dependent single-frequency dielectric model was developed for frozen mineral soils on the base of dielectric measurements of three soils with clay content 9.1%, 20.6%, and 41.3%. The model provides the CRPs of the frozen mineral soils as a function of dry soil density, moisture, texture (clay content), and temperature. The model was validated by the good agreement with the measured data for the wave frequency of 1.4 GHz. To calculate the CRP of frozen soil as a function of moisture and temperature using formulas in (1)–(4), we should know: 1) dry soil density,  $\rho_d$  [g/cm<sup>3</sup>], and 2) clay content in soil,  $C\%$ . The developed dielectric model can be used in data processing algorithms for modern remote sensing missions, such as SMOS, SMAP, and Aquarius.

## ACKNOWLEDGMENT

The study was supported by a grant from the Russian Foundation for Basic Research (project No. 16-05-00572).

## REFERENCES

1. Mironov, V. L. and S. V. Fomin, “Temperature and mineralogy dependable model for microwave dielectric spectra of moist soils,” *PIERS Proceeding*, 938–942, Moscow, Russia, August 18–21, 2009.
2. Mironov, V., Y. Kerr, J.-P. Wigneron, L. Kosolapova, and F. Demontoux, “Temperature and texture dependent dielectric model for moist soils at 1.4 GHz,” *IEEE Geosc. Remote Sens. Letters*, Vol. 10, No. 3, 419–423, 2013.
3. Dobson, M. C., F. T. Ulaby, M. T. Hallikainen, and M. A. El-Rayes, “Microwave dielectric behavior of wet soil — Part II: Dielectric mixing models,” *IEEE Trans. Geosci. Remote Sensing*, Vol. 23, No. 1, 35–46, 1985.
4. Zhang, L., J. Shi, Z. Zhang, and K. Zhao, “The estimation of dielectric constant of frozen soil-water mixture at microwave bands,” *Proc. of IGARSS*, 2903–2905, Toulouse, France, July 21–25, 2003.
5. Mironov, V. L., Ya. Kerr, L. G. Kosolapova, I. V. Savin, and K. V. Muzalevskiy, “Temperature dependent dielectric model for an organic soil thawed and frozen at 1.4 GHz,” *IEEE J. Sel. Topics Appl. Earth Observ. Remote Sens. (JSTARS)*, Vol. 8, No. 9, 4470–4477, 2015.